INL/RPT-24-76318
Revision 0

Development of INL Ultrasonic Thermometer

January 2024

Joshua Daw
Bibo Zhong

Idaho National Laboratory

INL is a U.S. Department of Energy National Laboratory
operated by Batelle Energy Alliance, LLC

INL/RPT-24-76318
Revision 0

Development of INL Ultrasonic Thermometer

Joshua Daw
Bibo Zhong

January 2024

Idaho National Laboratory
Measurement Sciences Laboratory
Idaho Falls, Idaho 83415

http://www.inl.gov

Prepared for the
U.S. Department of Energy
Office of Nuclear Energy
Under DOE Idaho Operations Office
Contract DE-AC07-05ID14517

Page intentionally left blank

SUMMARY

This document summarizes the development of an ultrasonic thermometer (UT) at Idaho National Laboratory (INL). The UT is a temperature sensor capable of multi-point measurements at very high temperatures. All components of the UT have been improved over the course of this work. The base technology, a magnetostrictive transducer, has been shown to be highly radiation tolerant. The solenoidal coil used in the transducer was redesigned to operate at higher frequencies than were previously possible. Materials for the acoustic waveguide (i.e., the sensing portion of the device) have been tested and ideal candidates identified. Finally, a solution to the sticking issue (i.e., diffusion bonding between the waveguide and a protective sheath) has been developed and tested.

Page intentionally left blank

CONTENTS

FIGURES

TABLES

ACRONYMS

ATR	Advanced Test Reactor
INL	Idaho National Laboratory
MITR	Massachusetts Institute of Technology Research Reactor
SFR	sodium fast reactor
TRISO	tristructural-isotropic
ULTRA	Ultrasonic Transducer irradiation test
UT	ultrasonic thermometer

Page intentionally left blank

1. Introduction

New nuclear fuel, cladding, and structural materials carry the potential to enable safer, more economic energy from existing and advanced nuclear reactor designs. However, characterization of these materials under high-temperature, high-radiation conditions is limited by insufficient available data, and robust instrumentation is needed to evaluate the performance of candidate materials under such environments. Furthermore, the nuclear industry's reliance on computer models to predict component and system behavior under both normal and off-normal conditions surpasses the capability of current measurement techniques to measure physical phenomena with sufficient resolution. Validation of these simulations against experimental data is necessary for obtaining regulatory approval, and new sensors and measurement techniques are required in order to facilitate this validation. Testing of new high-performance fuels and materials for advanced reactor designs necessitates sensors capable of operating under conditions unsuitable for commonly used temperature sensors (e.g., exposure to temperatures exceeding 2000°C in gases or corrosive environments such as liquid metals or molten salts). Given the recent push to develop advanced reactors—making such conditions increasingly common—advanced methods for measuring temperatures and temperature profiles by employing chemically compatible sensors are now of even higher priority. In this regard, the ultrasonic thermometer (UT) represents a versatile technology that can be adapted to such types of extreme conditions.

The UT is based on the principle that the speed of sound traveling through a material (i.e., acoustic velocity) is dependent on the temperature of the material. For an acoustically thin rod (diameter of less than ~0.1 wavelength [1]) operating in a longitudinal wave mode, the velocity (v) is a function of the elastic modulus (E) and material density (ρ), both of which are functions of temperature (T) (see Eq. 1):

$$v(T) = \sqrt{\frac{E(T)}{\rho(T)}} \tag{1}$$

Temperature may be derived by introducing a short acoustic pulse to the sensor and measuring the time delay of the acoustic reflections generated at acoustic discontinuities along the sensor length. Typically, these discontinuities are created by machining notches into the sensor rod. UTs can be made to have very small diameters yet still maintain a high level of durability, as the sensor consists simply of a small-diameter metallic rod or wire (though a sheath may also be required) [2]. Nor is any electrical insulation needed in the sensor. Electrical insulation, required for thermocouples, can degrade when subjected to high temperatures (>1800°C), causing shunting errors. The UT can measure temperatures nearing the melting point of the sensor material, enabling monitoring of temperatures potentially in excess of 3000°C. The primary appeal of the UT is its potential for real-time in-core temperature profile measurements using a single multi-segment sensor. Figure 1 shows a conceptual design for a multi-segment UT, with the key components identified.

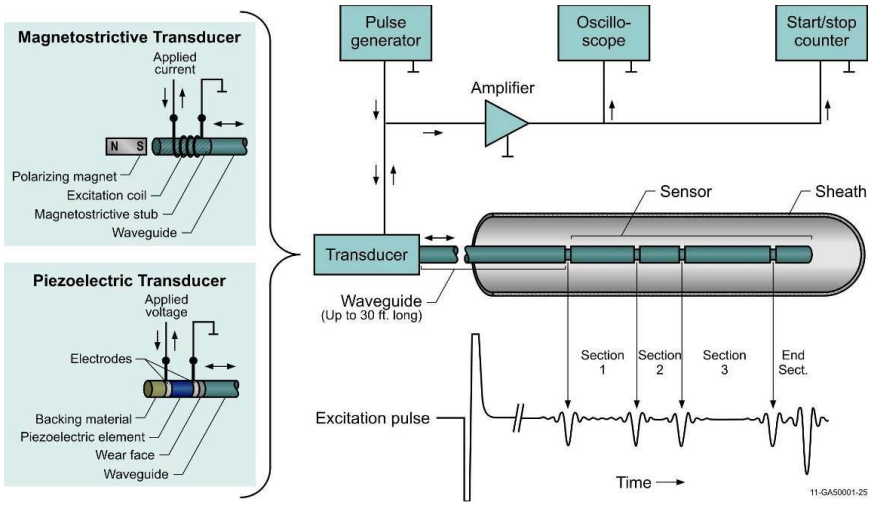

Figure 1. Basic schematic diagram of a UT.

Development of the UT at Idaho National Laboratory (INL) has focused on high-temperature operation and inherent radiation tolerance. Thus, its specific components and design features were developed with these aspects in mind.

2. Background

Improvement of characterization and monitoring the evolution of nuclear fuel and material evolution has become necessary, especially in anticipation of the development of advanced reactor designs and the need to qualify these along with designs for newer fuels, coolants, and structural materials. Ultrasonic measurement, with its longstanding and successful history in materials characterization, including the detection and characterization of degradation and damage [3], logically plays a pivotal role in this context. Post-irradiation examinations have logically revealed correlations between fuel microstructural parameters, such as porosity and grain size, and ultrasonic velocity [4]. Frequency requirements for such measurements are generally constrained to values greater than 10 MHz [5]. However, lower frequencies can logically be employed for specific applications such as ultrasonic thermometry, where the frequency requirements may logically be 100–150 kHz or lower [1].

Table 1 lists typical test/operating temperatures expected for various fuel and cladding materials, as well as the temperature accuracy and axial spatial resolution thought to be needed.

Table 1. Summary of desired fuel temperature measurements for irradiation testing.[a]

Parameter	Representative Peak Value	Desired	
		Accuracy	Spatial Resolution
Fuel Temperature	Ceramic Light-Water Reactor: 1400°C	2%	1–2 cm (axially), 0.5 cm (radially)
	Ceramic Sodium Fast Reactor (SFR): 2600°C		
	Metallic SFR: 1100°C		
	Tristructural-isotropic (TRISO) High-Temperature Gas-cooled Reactor: 1250°C		
Cladding Temperature	Ceramic Light-Water Reactor: <400°C	2%	1–2 cm (axially)
	Ceramic SFR: 650°C		

[a] The representative peak values, accuracy, and resolution are based on the engineering judgement of relevant experts.

	Metallic SFR: 650°C		

2.1 Prior Development

Development of ultrasonic-waveguide-based thermometers began in the 1960s. Their initial application was to measure temperatures in nuclear thermal rockets [6]. Eventually, they were utilized to measure high temperatures in nuclear fuels tests such as the fuel failure tests conducted at INL in the Transient Reactor Test Facility (TREAT), Loss of Fluids Test, and Power Burst Facility with a significant amount of research and development toward their use in steady-state reactors [7-16]. Development proceeded within various organizations on into the early 1980s, and has continued in sporadic fashion ever since. The UT never became an accepted standard temperature sensor, as the electronics and signal processing were largely beyond the technological capabilities available at the time. Among the major issues associated with UT deployment for irradiation testing were selecting appropriate sensor materials for very-high-temperature applications, eliminating contact bonding (sticking), and signal processing. Only limited signal processing technology was available back when the prior work was conducted, and variations between different research efforts are not well described. The major results of previous research pertain to the testing of various sensor materials and to methods for reducing sticking. Table 2 summarizes the results of prior UT testing in irradiations conducted at various organizations.

Table 2. Summary of prior UT irradiation testing [17].

Organization	Test	Max. Temperature	Sensor Material	Comments
INL	WDC-3-5 Engineering Test Reactor	2707°C	W-25%Re	Minor sticking between the sensor and sheath
INL	Power Cooling Mismatch	2017°C	Thoriated Tungsten	Short duration tests, no failures
INL	Capsule Driver Core	~1807°C	W-25%Re	Demonstrated a faster response time than thermocouples
Oak Ridge National Laboratory	High Flux Isotope Reactor-HRB	907–1107°C	Rhenium	-1070°C drift after test, due to transmutation of rhenium
Sandia National Laboratories	Molten Fuel Pool	2860°C	Thoriated Tungsten	Five sensor segments in molten UO_2, thoria sheath; maximum temperature reached in 19 minutes
Nuclear Research and Consultancy Group	RETSON	2000°C	Thoriated Tungsten	2000-hour test at 2000°C resulted in less than 30°C decalibration
Commissariat à l'énergie atomique/Ispra	FARO	2800°C	Doped Tungsten	Operation for over 1 hour in oxide corium

Commissariat à l'énergie atomique	PHEBUS FPT3	2207°C	Thoriated Tungsten	Transients in excess of 300°C/min experienced

Table 3 and Table 4 show the results of testing different sensor materials and proposed solutions to the sticking problem, respectively.

Table 3. Waveguide material testing summary from previous research efforts.

Waveguide Material	Result
Rhenium	High sensitivity. High-temperature operation demonstrated to 3180°C. Rapid decalibration due to transmutation.
Tungsten	High-temperature operation demonstrated to 2860°C. Rapid decalibration due to transmutation.
2% Thoriated Tungsten	High-temperature operation demonstrated to 2860°C. Rapid decalibration due to transmutation.
AKS-Tungsten	High-temperature operation demonstrated to 2860°C. Rapid decalibration due to transmutation.
Tungsten-25%Rhenium	High-temperature operation demonstrated to 2650°C. Rapid decalibration due to transmutation.
Molybdenum	Tested to 1800°C. Low attenuation observed. Not thoroughly tested due to low melting temperature and similar sensitivity when compared to tungsten.
Niobium	Flat, non-singular calibration curves.
Tantalum	Results not reported.
Platinum	Non-reproducible calibration curve. High attenuation.
Graphite	Results not reported.
Stainless Steel 302	Good performance to 1200°C. High temperature sensitivity. Spurious reflections between 1200°C and 1300°C attributed to annealing of cold work from wire drawing.
Nickel	Significant changes in calibration curve between cycles.
Titanium	Good performance to approximately 900°C. Low attenuation. High temperature sensitivity. A phase change precludes the use of titanium sensors at above 880°C.
Vanadium	Non-reproducible calibration curve. Significant embrittlement.
Rhodium	Good performance to 1300°C. Very high thermal neutron absorption cross section.
Zirconium	Good performance to 860°C. Not useful above 860°C due to phase change.

Table 4. Results of prior attempts to mitigate sticking.

Sticking Reduction Strategy	Result
Thoria Coating/Sheath	Effective to 2400°C. At above 2400°C, vaporization of thoria, migration of vapor to cooler regions, and deposition onto waveguide cause total loss of signal.
Stand-Off Reflectors	Effectiveness not commented on.
Tensioned Waveguide	Effectiveness not commented on.

Wire Cloth	Identified as the most effective method.
Rotating Waveguide	Increases sticking due to friction welding.
Ribbed Sheath	Deemed impractical to fabricate.
Threaded Waveguide	Increases sticking due to contact pressure.
Wire Wrapped around Waveguide	Increases sticking due to contact pressure.

The results of previous development reveal several areas that require improvement before the UT can be adopted as standard technology for monitoring temperatures in irradiation experiments and advanced reactors. Given the advancement of data acquisition systems and signal-processing technologies, the necessary improvements will primarily center on identifying the best waveguide materials, determining a practical means of eliminating sticking, and demonstrating the required level of radiation tolerance.

3. Development History

The following sections report INL's development advances for the different components of the UT.

3.1 Magnetostrictive Transducer

Magnetostrictive materials typically consist of magnetic metals and alloys. Magnetostriction is a phenomenon in which a material undergoes a change in shape under the influence of an externally applied magnetic field. All magnetic materials are magnetostrictive, but most are not useful because their magnetostrictive effect is very slight. The magnetostrictive transducer is basically identical to a ferritic core solenoidal field coil [1], except that the magnetic permeability of the core undergoes significant changes as a function of the stress state of the material. As such, the coil is used to both generate and receive acoustic signals passing through the core by means of non-contact electromagnetic coupling. The basic concept of magnetostriction is illustrated in Figure 2.

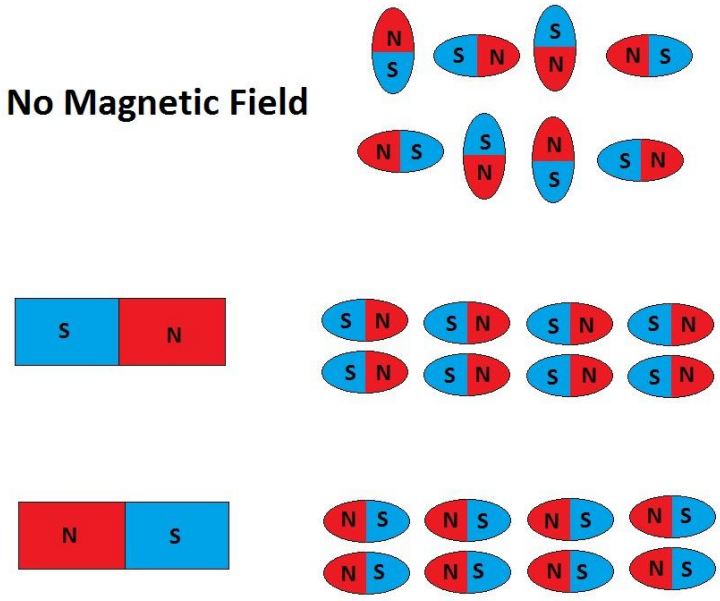

Figure 2. Magnetic domain alignment as a function of externally applied magnetic field.

The utilization of magnetostrictive transducers in test reactors has been proposed for measuring temperature [7,18], liquid level, density, flow, pressure, boiling occurrence, bubble location, and acoustic emissions [19]. The mechanical coupling achieved through direct welding or brazing, coupled with the enhanced generation of guided wave modes, renders magnetostrictive transduction particularly suitable

for low-frequency measurements, such as ultrasonic thermometry [19]. Beyond approximately 200 kHz (a typical operating frequency for magnetostrictive transducers), ultrasonic waves in 1.5 mm diameter waveguides (a standard diameter for temperature sensors) exhibit dispersion. This phenomenon causes the waves to transition from primarily extensional to shear, flexural, etc. Since each wave mode travels at a different speed, analyzing the received signals becomes increasingly challenging. Additionally, higher-frequency waves experience more rapid attenuation as they interact with smaller features like grain boundaries. This challenge is accentuated at elevated temperatures, given that acoustic attenuation is temperature-dependent.

Properties crucial for in-pile measurements include maximum operating temperature, sensitivity, and resistance to radiation damage. Unlike piezoelectric materials, magnetostrictive materials consist mainly of elemental metals or alloys. Consequently, the effects of radiation on metals differ significantly from those on ceramics. For instance, investigations into magnetic Fe-Ni alloys like Permalloy indicate a decrease in magnetic permeability with neutron irradiation, attributed to domain immobilization from point defects generated by displacement cascades [21]. This limitation is believed to affect the magnetostrictive capabilities of the material, although magnetostrictive effects have been reported at fluences as high as 5×10^{19} n/cm² [18]. The magnetostrictive materials considered for testing fall into three categories: pure metals (nickel, iron, and cobalt), alloys (formed by combining pure magnetostrictive materials with other alloying materials), and "giant" magnetostrictive materials with significantly improved responses. Metallic magnetostrictive materials easily couple with a metallic waveguide via welding, overcoming acoustic coupling challenges associated with piezoelectric materials. Waveguide materials of interest have acoustic impedances similar to common magnetostrictive materials, facilitating efficient acoustic coupling to a cylindrical waveguide using a magnetostrictive rod or wire of appropriate diameter. Since signals are transferred electromagnetically (non-contact), the coil can be a separate component, enhancing sensor robustness by isolating it from the environment. The initial development of the INL UT involved assessing the radiation tolerance of potential transducer active materials through funding from the U.S. Department of Energy Advanced Sensors and Instrumentation program and the Nuclear Scientific User Facilities [22].

3.1.1 Ultrasonic Transducer Irradiation Test

The Ultrasonic Transducer irradiation test (ULTRA) was a collaborative effort involving INL, Pacific Northwest National Laboratory, Argonne National Laboratory, the Pennsylvania State University, the Massachusetts Institute of Technology, and the French Alternative Energies and Atomic Energy Commission. Transducer performance during irradiation is a significant issue that must be addressed prior to in-core deployment of ultrasound-based sensors, and this test helped to do so by evaluating candidate materials capable of generating and receiving ultrasonic waves after exposure to high neutron fluences. A test capsule design was developed that included both piezoelectric and magnetostrictive materials, transducers, and sensors. Test conditions were selected that exceeded the fluences evaluated in prior ultrasonic transducer irradiations.

The tank-type Massachusetts Institute of Technology Research Reactor (MITR) [23] is currently licensed for 6 MW operation. Figure 3 shows the MITR, its test position, and the ULTRA capsule, which was inserted into the reactor core at a location where the thermal flux was approximately 3.6×10^{13} n/cm^2-s and the fast flux (energy > 0.1 MeV) was 1.2×10^{14} n/cm^2-s. Geometric constraints in the in-core experiment tube limited the test capsule dimensions to 46 mm in diameter and 610 mm in length. It was proposed that the test exceed the fast neutron fluences of prior piezoelectric transducer irradiations (e.g., $> 1 \times 10^{21}$ n/cm^2 at energy > 1.0 MeV). To observe rapid changes at relatively low fluences, the test was started with the reactor coming to power slowly, enabling data collection at low fluence levels where failures were observed in prior piezoelectric transducer irradiations. The expected steady-state fast flux (energy > 1 MeV) was 3.5×10^{13} n/cm^2-s with the reactor running at 5.8 MW power.

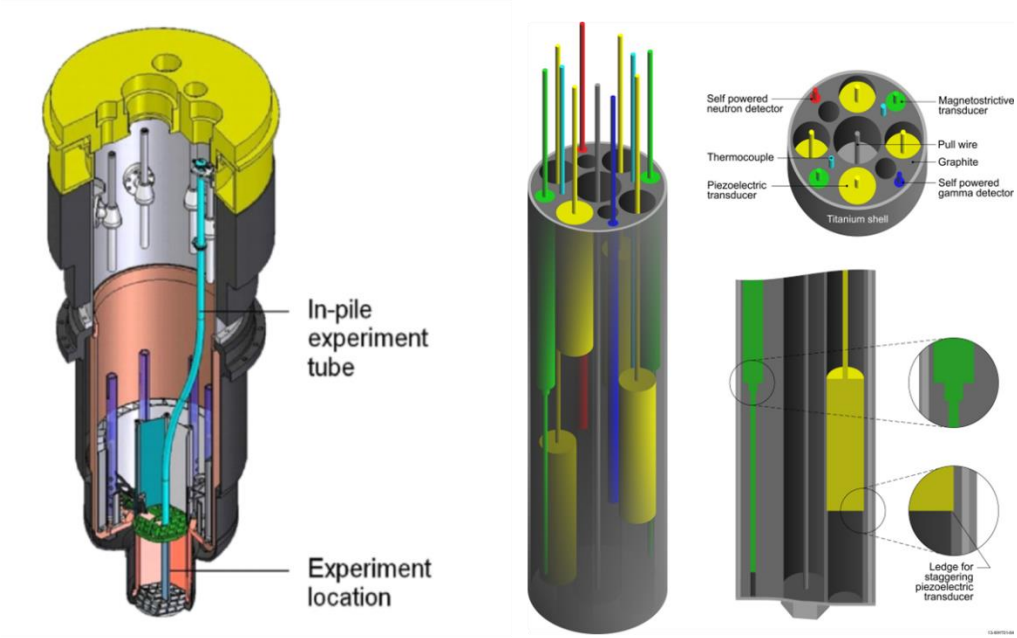

Figure 3. Images of the MITR, showing the test position, and the ULTRA test capsule.

The magnetostrictive materials (i.e., Remendur and Galfenol) included in the ULTRA experiment were chosen for their saturation magnetostriction, high Curie temperature, availability, etc. Figure 4 shows the magnetostrictive transducer design applied to the ULTRA experiment. (However, the biasing magnets were deemed unnecessary and thus were not used).

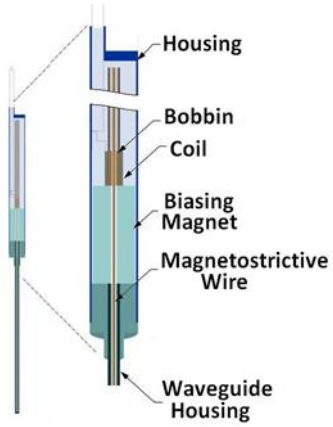

Figure 4. Magnetostrictive transducer design for the ULTRA irradiation experiment.

Figure 5 shows the normalized amplitude for the Remendur transducer as a function of accumulated fluence. The green trace corresponds to the reactor power history. A general decreasing trend is seen, but signal recovery after temperature transients indicates that some of the signal attenuation is due to temperature effects—in this case, binding of the wire against the coil bobbin.

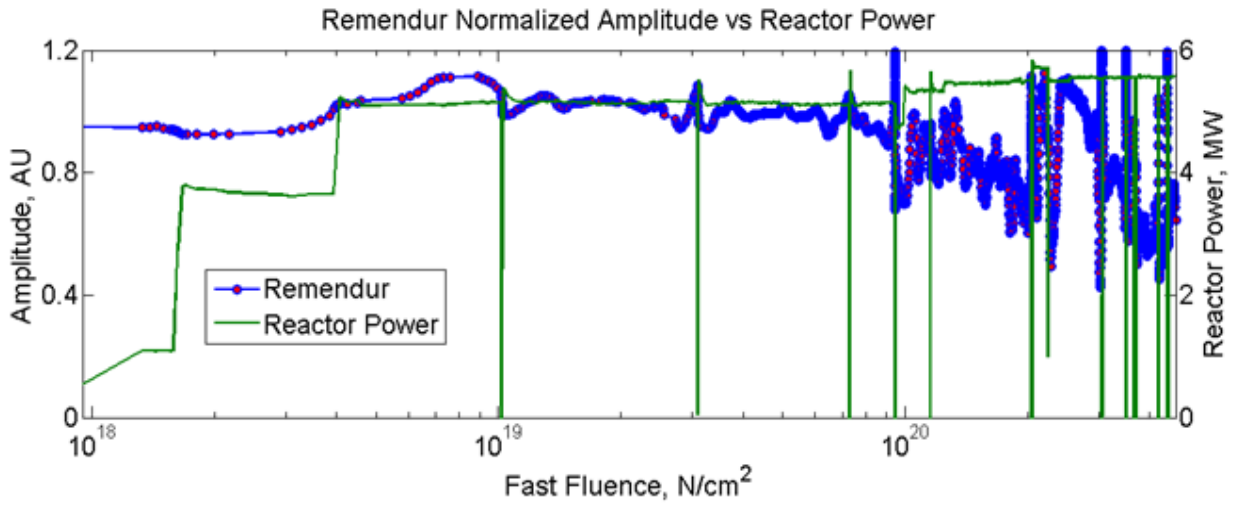

Figure 5. Remendur transducer normalized amplitude as a function of total fast fluence.

The Galfenol transducer demonstrated very stable operation over the course of the irradiation, though its total peak-to-peak signal amplitude was typically on the order of one third that observed for Remendur. Figure 6 shows the normalized peak-to-peak amplitude for the Galfenol transducer as a function of accumulated fluence. The decreases in signal strength observed when reactor power was increased appear to result from increases in operating temperature, as the signal strength stabilizes shortly after each power increase.

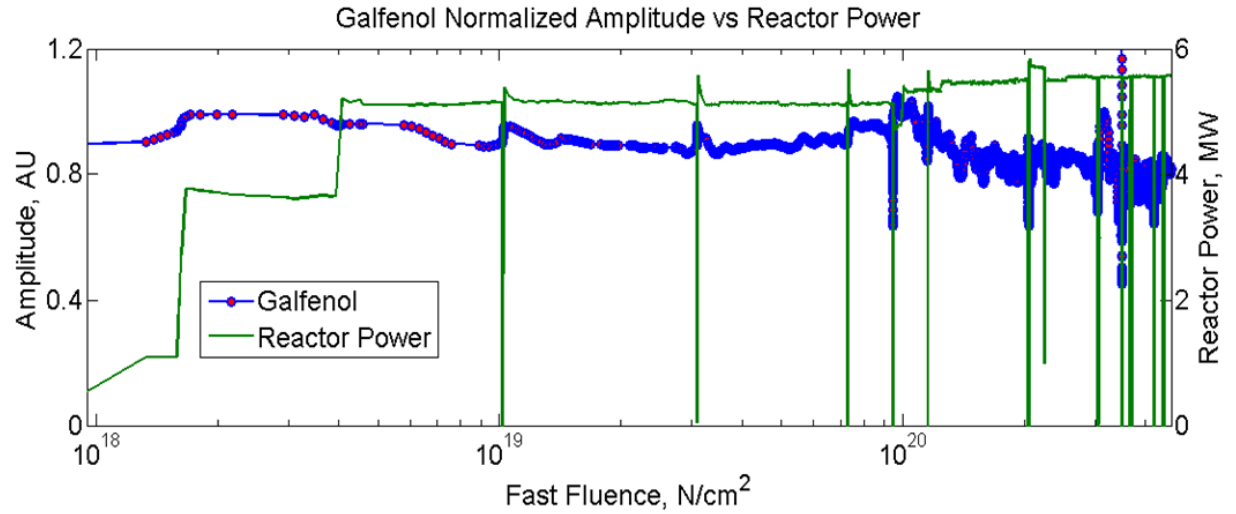

Figure 6. Galfenol transducer normalized amplitude as a function of total fast fluence.

The ULTRA experiment reached a total fast fluence of 8.8×10^{21} n/cm^2. Post-irradiation testing of the irradiated samples showed no residual effects of irradiation. The measured signal amplitude of the irradiated materials did not significantly differ from that of unirradiated samples. Though several piezoelectric materials (e.g., aluminum nitride and bismuth titanate) showed promise after being tested, the tested magnetostrictive materials were observed to have high radiation tolerances and have been used in the UT development, as such high radiation tolerance levels enable the UT transducer to be placed within the reactor pressure vessel, eliminating the need for complicated pressure boundary feedthroughs.

The metallic magnetostrictive materials are also easily coupled to a metallic waveguide via welding, eliminating most of the acoustic coupling challenges associated with piezoelectric materials.

Through the present work, a new coil design was created that operates at higher frequencies than are typical for magnetostrictive transducers. This patented design essentially consists of a series-connected chain of small coils wound sequentially in opposition. This coil effectively causes the enclosed sections of magnetostrictive materials to alternately pinch and expand, generating higher frequency (~2 MHz) acoustic waves yet still retaining sufficient signal amplitude thanks to constructive interference. Figure 7 shows this concept, along with a high-temperature coil wrapped on a bobbin fabricated from alumina via additive manufacturing.

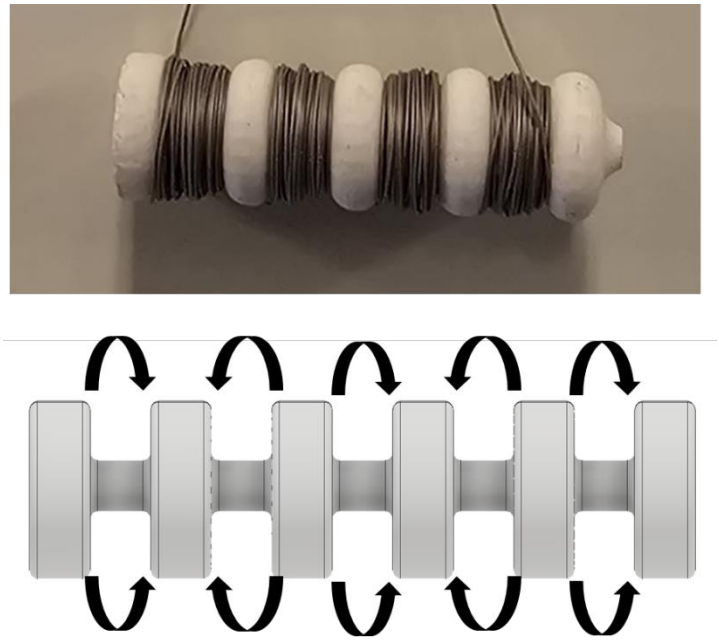

Figure 7. High-temperature, high-frequency coil for the magnetostrictive transducer.

Figure 8 shows the waveforms captured for both a low-frequency (200 kHz) and a high-frequency (1 MHz) coil coupled to waveguides featuring five reflectors each spaced 1 cm apart. It is clear that although the low-frequency coil cannot resolve such closely spaced reflectors, the high-frequency coil can.

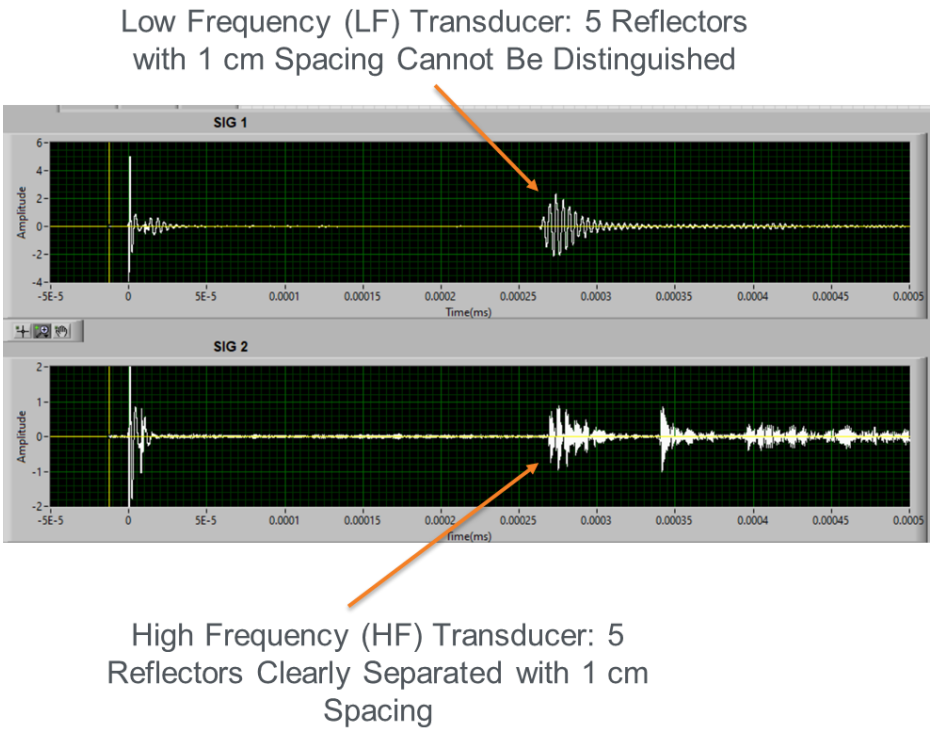

Figure 8. Spatial resolution difference comparison between the low- and high-frequency coils.

3.2 Waveguides

3.2.1 Materials

Based on prior research, two "standard" waveguide materials were selected for application to the UT. For temperatures below 1000°C, stainless steel (304 or 316) are ideal, as they have good sensitivity, low attenuation, low neutron interaction, and good corrosion resistance. For these same reasons, Inconels are a good choice as well. For higher temperatures, molybdenum—or lanthanated molybdenum—is the best choice, though its corrosion resistance and sensitivity are not as good. Other materials have been tested and may be better suited for certain applications. Table 5 lists the results of the materials testing at INL.

Table 5. Summary of UT waveguide materials tested at INL.

Material and Diameter	Maximum Temperature Tested	Comments
1.6 mm Stainless Steel 316	~1380°C	Excellent performance. High temperature sensitivity. Tested to melting point, phase change obvious via acoustic signal.
0.25 mm Stainless Steel 316	1050°C	Excellent performance to 1000°C, then attenuation becomes excessive. High temperature sensitivity.
0.25 mm Inconel 606	800°C	Excellent performance. High temperature sensitivity.
0.25 mm Titanium	800°C	High temperature sensitivity. Solid-state phase change at ~880°C will make calibration above this temperature non-singular.

0.25 mm Zircaloy 4	1050°C	Sticking and attenuation issues starting at 800°C. High temperature sensitivity. Solid-state phase change at ~1100°C will make calibration above this temperature non-singular.
0.25 mm Zirconium	800°C	High temperature sensitivity. Solid-state phase change at ~1100°C will make calibration above this temperature non-singular.
0.5 mm Platinum	800°C	Excessive attenuation. Very noisy signal due to the high acoustic impedance mismatch with magnetostrictive material.
0.25 mm Niobium-1% Zirconium	1300°C	Flat calibration curve, with initial increase in the speed of sound leading to non-singular calibration curve for temperatures below ~500°C.
0.25 mm 85% Silver-15% Palladium	800°C	Excessive attenuation. Very noisy signal due to the high acoustic impedance mismatch with magnetostrictive material.
1.6 mm Molybdenum	~2500°C	Excellent performance to the maximum temperature limit of furnace. Low temperature sensitivity.
0.25 mm Molybdenum	1800°C	Excellent performance to ~1400°C. Excessive attenuation of signal at 1500°C. Low temperature sensitivity.
0.25 mm Tantalum	800°C	Excellent performance. Low speed of sound is good for temperature resolution. High neutron capture cross section.
1 mm Tungsten	~2500°C	Excellent performance to the maximum temperature limit of furnace. High neutron capture cross section.

3.2.2 Reflector Types

The classical UT design consists of a solid rod (over 1 mm in diameter), with a notch, diameter change, or other feature being used as the source of segmentation and acoustic reflections. The solid rod has certain advantages over the multi-waveguide design. First, the fact a sheath is typically unnecessary can reduce problems caused by sticking. Second, a larger-diameter waveguide is less sensitive to external factors such as pressure feedthroughs, as comparatively less acoustic energy propagates at the waveguide outer surface. Figure 9 shows a waveguide with a notch-style reflector.

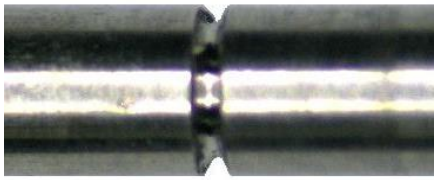

Figure 9. Notch cut into a 1.6-mm-diameter waveguide.

Smaller waveguides (on the order of 1/10th of the acoustic wavelength, with 0.25 mm being typical) are advantageous, as there tends to be less acoustic dispersion (for similar operational frequencies) than with larger waveguides, leading to a higher-amplitude signal with a better signal-to-noise ratio. However, they are more sensitive to external factors and are more prone to sticking. Attenuation has also been observed to be higher in smaller waveguides. For these smaller waveguides, reflectors typically take the

form of bumps of the waveguide material welded onto the waveguide. Sharp double bends in the waveguide also work, but tend to add mode-converted flexural waves that may interfere with signal processing. Figure 10 shows such reflectors utilizable for small-diameter waveguides.

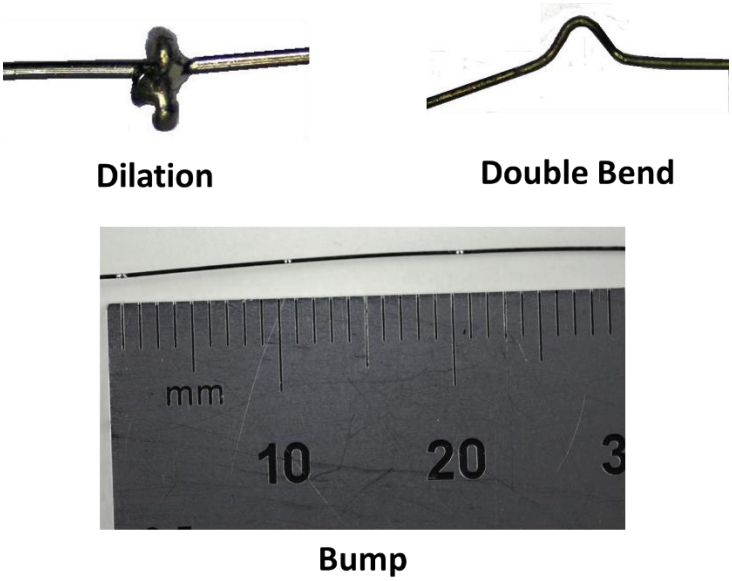

Figure 10. Reflective features that can be utilized in small-diameter waveguides.

Multi-waveguide UTs, in which sensor segmentation is accomplished using several small-diameter wires of different lengths, could potentially improve UT performance by reducing the higher-order reflections observed when using a single waveguide with multiple echogenic features along its length. Figure 11 shows images of a multi-waveguide bundle.

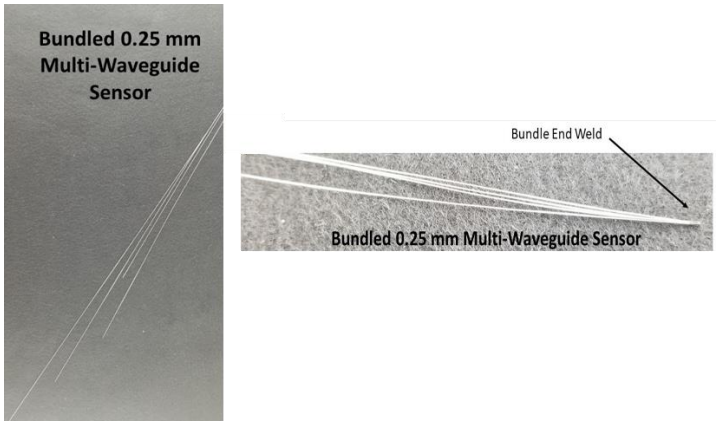

Figure 11. Multi-waveguide bundle: (left) sensor section with waveguides of different lengths; (right) magnetostrictive bundle.

3.2.3 Sticking

Although the sticking issue has already been addressed in previous research, an ideal solution was never identified. Recently, INL retested some of the previous solutions and developed a brand-new method. Among the prior methods was the use of small-diameter wire wrapped around the waveguide. In that particular case, the waveguide was molybdenum and the wrap wire was a tungsten-rhenium thermocouple wire, the idea being to minimize the likelihood of diffusion by using a wrap wire featuring

a significantly higher melting temperature. Another previously tested option was the use of bump-style reflectors as stand-offs. Advances in micro-laser welding technology were thought capable of potentially improving this method. Newer methods included using a ceramic tube to isolate the waveguide from the sheath, and using a printed ceramic spacer designed to minimize contact between the waveguide and the sheath. Figure 12 shows x-ray images of the different methods.

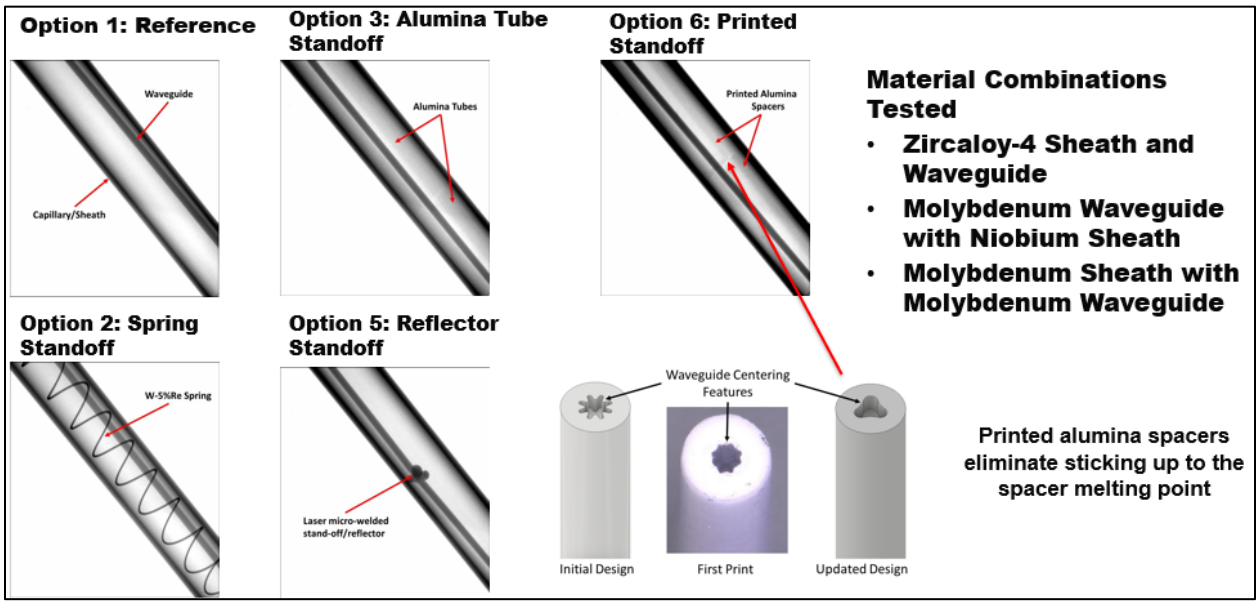

Figure 12. Methods of reducing the occurrence of sticking between the UT waveguide and the sheath.

The wire wrap produced the same result as before, making the sticking problem worse due to the contact forces being high. The stand-off reflectors were also unsuccessful. This is because laser welding the bumps onto the waveguide always created a bend in it, pressing the waveguide into the sheath a small distance from the bumps and increasing the contact force, which in turn increased the diffusion bond potential. Furthermore, the alumina tube reduced the inner diameter of the sheath, causing binding of the waveguide. This, though not strictly "sticking" per se, produces the same effect on signals. On the other hand, the printed ceramic spacers successfully eliminated sticking at up to the spacers' melting point (in this case, just over 2000°C for aluminum oxide).

3.3 Updated Design

Figure 13 shows an updated general schematic of the UT. This updated version utilizes a mineral-insulated coaxial cable (either 1 or 1.6 mm in diameter) with a stainless-steel sheath, stainless-steel housing, and a sensor sheath fabricated from whatever material was used for the sensor (typically stainless steel or molybdenum). Typical diameters of the housing and the sheath are 12.5 and 1.6 mm, respectively. The lengths of each section and the number of measurement zones can be tailored to the application (with as many as 15 segments having been demonstrated). To date, this is the most standardized version for use in irradiations.

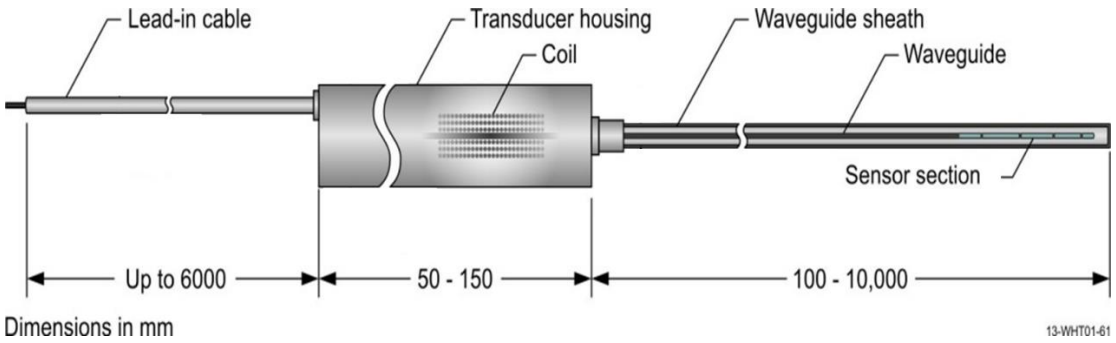

Figure 13. Updated UT diagram.

4. Deployment in Irradiation Experiments

The UT has been utilized in two irradiation experiments to date, with several others currently planned. This section summarizes the results of the completed irradiations.

4.1 ULTRA2

As a follow-up to the ULTRA irradiation, a follow-on irradiation funded by the Nuclear Scientific User Facilities was performed at the MITR. This experiment, called ULTRA2, was designed similarly to the original ULTRA experiment, except that active temperature control was employed to maintain the target temperature of ~650°C. The test included both UTs and fiber optic temperature sensors. Three UTs were tested: one used a commercially pure titanium waveguide sensor with a single measurement zone; the other two used Inconel 606 sensors, one with a single measurement zone and one with three. The results are summarized below.

Figure 14 shows the normalized delay time of the single-segment Inconel sensor and temperature measured by thermocouples. The data during initial reactor startup were unusable, possibly because the sensor's wiring may have suffered a mechanical pinch that cleared up after temperature cycling. The signal followed the reactor temperature well for most of the test. However, some intermittent signal loss was observed over the last few reactor cycles, evidencing that the coil was the component that failed, as failure of any other component would not allow for recovery.

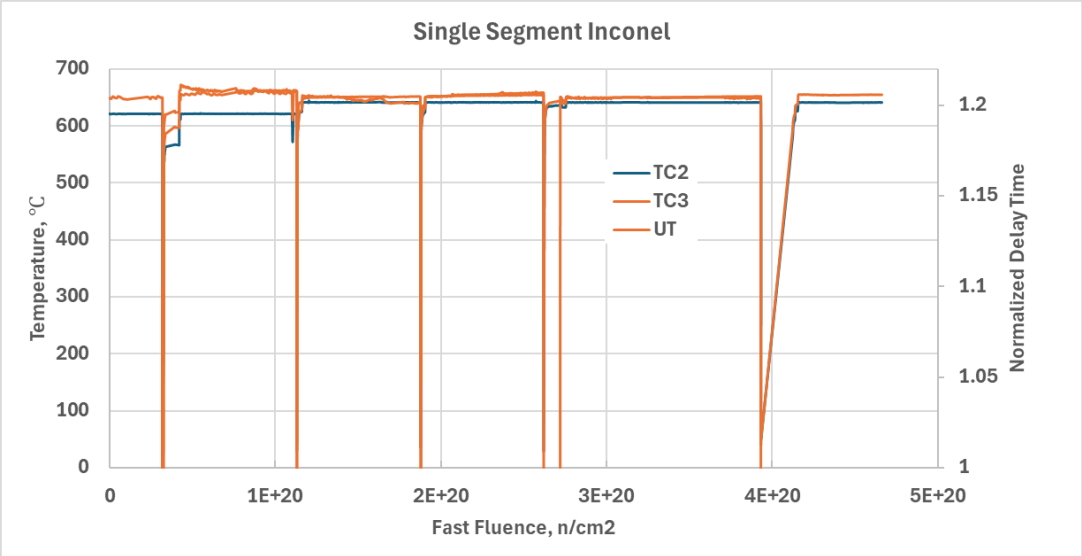

Figure 14. Single-segment Inconel sensor results.

Figure 15 shows the normalized delay time of the three-segment Inconel sensor and temperature measured by thermocouples. As with the single-segment sensor, the signal closely matches the reactor temperature throughout most of the irradiation. Some anomalous behavior was observed during the early part of the irradiation, seen as an opposing response between the first and second segments (as one signal increased, the other decreased in direct proportion). It is unclear at this point whether this was a physical phenomenon or an artifact of the signal acquisition process. This sensor also failed intermittently before finally irrevocably failing after ~7000 hours.

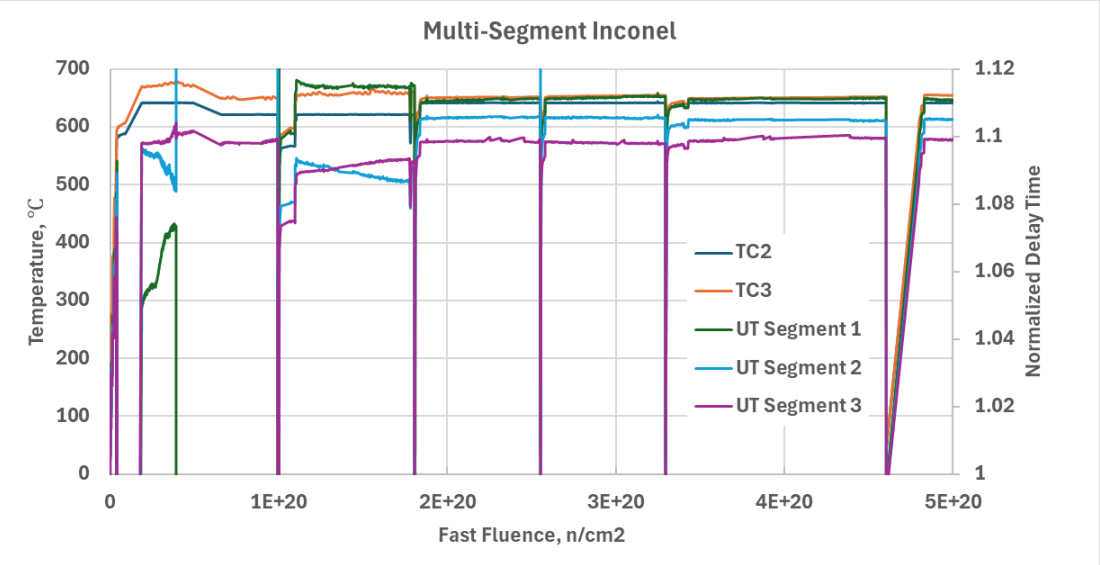

Figure 15. Three-segment Inconel UT results.

Figure 16 shows the normalized delay time of the single-segment titanium sensor, which performed well for almost 3000 hours prior to undergoing failure, and temperature measured by thermocouples. Unlike with the Inconel sensors, a slow decrease was observed in the measured delay time, likely because fast neutron damage caused a slow increase in the Young's modulus of the titanium. Though the effect appears to have saturated by the last operational reactor cycle, this behavior may make titanium a poor material for use in UTs.

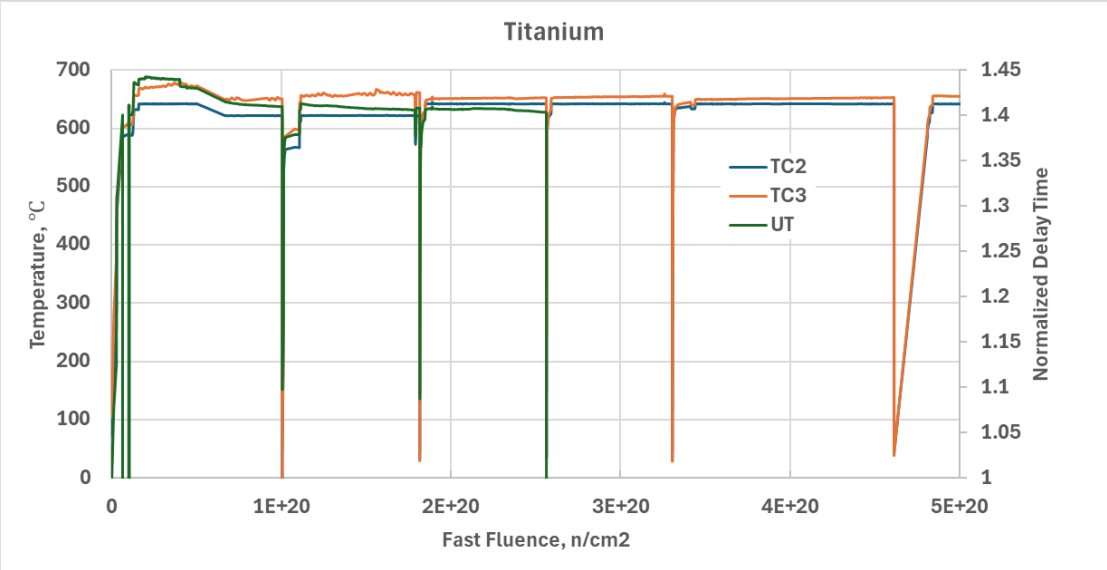

Figure 16. Single-segment titanium UT results.

4.2 Advanced Gas Reactor-5/6/7

The Advanced Gas Reactor-5/6/7 irradiation was the last in a series of experiments conducted at INL's Advanced Test Reactor in support of the development and qualification of TRISO low-enriched fuel for use in high-temperature gas-cooled reactors. A single-measurement-segment molybdenum UT was included in this experiment as a supplemental instrument for evaluating the UT's performance in the Advanced Test Reactor. The UT was placed in close proximity to several type K thermocouples used to monitor the operating temperatures of several self-powered neutron detectors. Figure 17 plots the temperature of the UT and nearby thermocouples. The differences in temperature magnitudes and short-term temperature trends are due to different local heating and cooling conditions. The UT closely follows the trends of the thermocouples. As with the ULTRA2 experiment, the eventual loss of signal is thought to be caused by failure of the coil. In both cases, the coil was fabricated from silver-palladium wire with a ceramic insulation that must be heat treated after winding. This wire becomes somewhat brittle after the heat treatment. Repeated temperature transients during reactor startup and shutdown likely caused the wire to break.

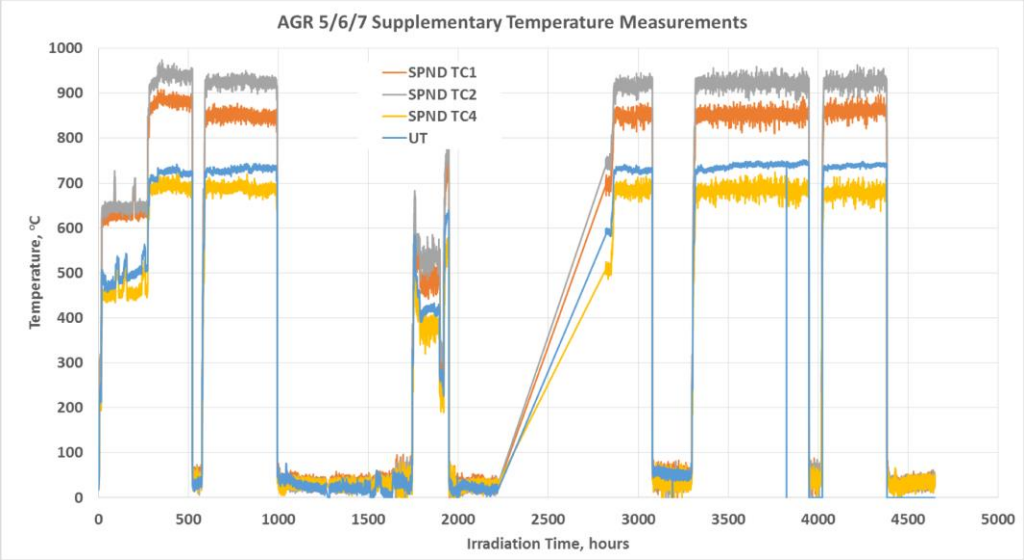

Figure 17. Temperature measured by the molybdenum UT, as compared with the measurements from nearby thermocouples, during the Advanced Gas Reactor-5/6/7 irradiation test.

5. Conclusions and Recommendations for Future Work

The UT development at INL has built on previous research, utilizing newer materials and fabrication methods to advance the design so that it may be deployed in irradiation experiments or advanced reactors at higher temperatures and fluences than were previously possible. This resulted in a design that has a standardized form but is still flexible in that the materials and sensor waveguide configurations can be selected for specific applications. Follow-on work should include further investigation of waveguide materials, as new materials are constantly being discovered/developed, and may allow for even higher-temperature operation. The printed spacers developed in this work could also be enhanced with ceramics featuring higher operating temperatures. Newer piezoelectric materials with high radiation tolerances could replace the magnetostrictive transducer currently in use and increase the operating frequency, thus benefitting UTs with short waveguides (where attenuation is non-problematic) and closely spaced reflectors.

6. References

1. Lynnworth, L.C., Ultrasonic Measurements for Process Control: Theory, Techniques, Applications, Academic Press, 1989.
2. J.E. Daw, J.L. Rempe, J.C. Crepeau, "Update On Ultrasonic Thermometry Development At Idaho National Laboratory," *8th International Topical Meeting on Nuclear Plant Instrumentation, Control, and Human-Machine Interface Technologies 2012*, NPIC and HMIT 2012: Enabling the Future of Nuclear Energy, 2012.
3. D. Ensminger, and L. J. Bond, Ultrasonics: Fundamentals, Technologies, and Applications, CRC Press, 2012.
4. K. Phani, et. al, "Estimation of Elastic Properties of Nuclear Fuel Material Using Longitudinal Ultrasonic Velocity - A New Approach," J. Nucl. Mat., 366, 2007, pp. 129-136.
5. J. F. Villard, et. al.,"Acoustic Sensor for In-Pile Fuel Rod Fission Gas Release Measurement," IEEE Transactions on Nuclear Science, 58, 2011, pp. 151-155.
6. Lynnworth, L.C., Carnevale, E.H., "Final Report-Ultrasonic Temperature Measuring Device," NASA CR-72339, August, 1967.
7. Lynnworth, L.C., Carnevale, E.H., McDonough, M.S., Fam, S.S., "Ultrasonic Thermometry for Nuclear Reactors," IEEE Transactions on Nuclear Science, Vol. NS-16, P. 184-187 1968.
8. Lynnworth, L.C., "Use of Ultrasonics for High-Temperature Measurements," Presented at American Society for Nondestructive Testing Meeting, Boston, MA, Mar. 20, 1968.
9. Papdakis, E.P., Lynnworth, L.C., Patch, D.R., Carnevale, E.H., "Ultrasonic Thermometry in LMFBR Systems," Final Report NYO-3906-13, Panametrics Inc. 1972.
10. Arave, A.E., Meservey, R.H., "A High Temperature Ultrasonic Thermometer for Measuring Reactor Fuel Temperature," IN-1413, Idaho Nuclear Corporation, 1970.
11. Arave, A.E., Panisko, F.E., Christiansen, J.A., "High-Temperature Ultrasonic Thermometer In-Reactor Fuel Rod Centerline Temperature Test Results," ANCR-1091, Aerojet Nuclear Company, 1972.
12. Arave, A.E., "Comparison of Four Tungsten Alloys for Use as Ultrasonic Thermometer Sensors," ANCR-1225, Aerojet Nuclear Company, 1975.
13. Arave, A.E., Buchenauer, J., "Use of Tungsten-2% Thoria Ultrasonic Transmission Line and Sensor to Improve the Performance of High-Temperature Ultrasonic Thermometry," TREENUREG-1021, Idaho National Engineering Laboratory, 1976.
14. Tasman, H.A., Schmidt, H.E., Richter, J., Campana, M, Fayl, G., "The TRESON Experiments: Measurement of Profiles in Nuclear Fuels by Means of Ultrasonic Thermometers," High Temperatures- High Pressures, Vol. 9 pp. 387-406, 1977.
15. Carlson, G.A., Sullivan, W.H., Plein, H.G., "Application of Ultrasonic Thermometry in LMFBR Safety Research," SAND-77 1157, Sandia Laboratories, 1977. (Also: 1977 Ultrasonics Symposium Proceedings)
16. Carlson, G.A., Sullivan, W.H., Plein, H.G., Kerley, M., "An Ultrasonic Thermometry System for Measuring Very High Temperatures in Reactor Safety Experiments," SAND79-0621, Sandia Laboratories, 1979.
17. Laurie, M., Magallon, D., Rempe, J., Wilkins, S., Pierre, J., Marquié, C., Eymery, S., Morice, R., "Ultrasonic High Temperature Sensors: Past Experiments and Prospective for Future Use," Joint

International Symposium on Temperature, Humidity, and Moisture and Thermal Measurements in Industry and Science, Portorož, Slovenia, May 31 - June 4, 2010.

18. L.C. Lynnworth, “Nuclear Reactor Thermometry,” US Patent Application 3,597,316: 3 Aug 1971.
19. S.C. Rogers, G.N. Miller., “Ultrasonic Level, Temperature, and Density Sensor,” *IEEE Trans. On Nuclear Science,* 29 (1), 1982, pp. 665-668.
20. N. Gopalsami, A.C. Raptis, “Acoustic Velocity and Attenuation Measurements in Thin Rods with Application to Temperature Profiling in Coal Gasification Systems,” *IEEE Transactions on Sonics and Ultrasonics,* SU-31, 1984, pp. 32-39.
21. R.D. Brown, J.R. Cost, J.T. Stanley, “Effects of neutron irradiation on magnetic permeability of amorphous and crystalline magnetic alloys,” *J. Appl. Phys.*, 55, 1984, pp. 1754-1756.
22. J. Daw, J. Rempe, J. Palmer, P. Ramuhalli, R. Montgomery, Paul Keller, HT Chien, B. Tittmann, B. Reinhardt, “NEET In-Pile Ultrasonic Sensor Enablement-Final Report,” INL/EXT-14-32505, September 2014.
23. *MITR Users Guide Rev. 3 July 2012,* Massachusetts Institute of Technology, 2012.

Page intentionally left blank